RASĀYAN *J. Chem.*
Vol. 19 | No. 1 | 250-258 | January-March | 2026
ISSN: 0974-1496 | e-ISSN: 0976-0083 | CODEN: RJCABP
http://www.rasayanjournal.com
http://www.rasayanjournal.co.in

EXTRACTION AND CHARACTERIZATION OF HIGH-PURITY SILICA AND α-ALUMINA FROM NAPA SOIL (WEST SUMATERA, INDONESIA)

M. Mawardi[1,✉], I. M. Isa[4], Syamsurizal[2], O. Suryani[1], F. Mawardi[3], F. Ilmi[1], S. Yuswilia[1], and F. Amanda[5]

[1]Department of Chemistry, Universitas Negeri Padang-25173, Padang, Indonesia.
[2]Department of Biology, Universitas Negeri Padang-25173, Padang, Indonesia.
[3]Department of Chemistry, Faculty of Mathematics and Natural Sciences, Universitas Andalas, Padang 2516, Indonesia
[4]Department of Chemistry, Faculty of Science and Mathematics, Universiti Pendidikan Sultan Idris, Tanjong Malim 35900, Perak, Malaysia
✉Corresponding author: mawardianwar@fmipa.unp.ac.id

ABSTRACT

Napa soil (NS), a naturally abundant material from West Sumatra, Indonesia, presents significant potential as a sustainable raw source for advanced material synthesis due to its high silica and alumina content. This study focuses on the extraction and characterisation of high-purity silica and α-alumina from NS through a combined calcination–alkali fusion–hydrothermal acid process. Calcination at 750 °C effectively transformed crystalline phases into more reactive amorphous forms, enhancing the SiO_2 and Al_2O_3 content. Silica extraction using NaOH achieved optimum yield at 4M, producing a material containing quartz and cristobalite phases as confirmed by XRD and FTIR analyses, with particle sizes ranging from <14 nm to 134 nm observed under SEM. XRF analysis indicated a silica purity of 69.85% with minor alumina residues. Alumina extraction using HCl (1.0–2.5 M) achieved a maximum yield of 86.8% at 1.5 M, yielding α-alumina with a hexagonal corundum structure confirmed by XRD, Al–OH and Al–O vibrations in FTIR spectra, and agglomerated morphologies with heterogeneous porosity observed by SEM. TGA results supported the formation stability of α-alumina at 750 °C. These findings demonstrate that Napa soil can serve as a sustainable and low-cost precursor for producing high-purity silica and α-alumina suitable for applications in ceramics, catalysts, and environmental remediation. The study contributes to the valorisation of natural minerals in Indonesia and provides a scalable route toward developing advanced functional materials from locally available resources.

Keywords: Napa Soil, Silica Extraction, A-Alumina; Calcination, Hydrothermal Acid, Characterization, Advanced Materials

INTRODUCTION

Napa soil (NS) is a type of natural mineral in West Sumatra. Previous studies showed that the present material is alumina, specifically kaolin and a trace amount of quartz. NS has abundant reserves in several districts but remains largely unutilized on a laboratory or industrial scale. It contains significant amounts of silica (51.70% SiO_2) and alumina (41.52% Al_2O_3), along with 5.90% of other oxide compounds.[1] Silica and alumina can be extracted using solid-liquid methods. Silica solubility is very low at pH below 10 but increases at pH over 10, indicating high solubility under alkaline conditions, thus enabling extraction with alkaline solvents.[2] Silica extraction can be conducted by hydrothermal methods to speed up the reaction rate. The hydrothermal method involves single-phase or heterogeneous reactions in aqueous solutions at elevated temperatures (> 25 °C) and pressures around 100 kPa, enabling the direct crystallisation of ceramic materials from solution.[3] Silica originating from natural materials-such as NS formed through feldspar weathering-generally exists in an amorphous form and exhibits higher reactivity because it contains silanol (Si–OH) functional groups. Synthesis methods using biomass can involve several treatments, such as thermal processing in an oven, warm-water soaking and rinsing, or chemical

http://doi.org/10.31788/RJC.2026.1919475

processing with alkaline hydroxides (like NaOH or KOH), acidic reagents, or ionic liquid solvents.[4,5] This study used NaOH benchmarking material to obtain silica. NaOH facilitates the breakdown of chemical bonds in NS, enabling silicon to react with oxygen and form SiO_2 .[4] Alumina can be obtained from NS through either acidic or alkaline extraction.[5,6] In the acidic route, alumina is dissolved at elevated temperatures; However, this technique is seldom applied on an industrial scale because it requires expensive acid-resistant equipment and the prior removal of iron oxide. In contrast, the alkaline process involves heating NS with soda and lime at about 1200 °C, transforming silica into calcium silicate ($2CaO{\cdot}SiO_2$), which enables its separation from alumina.[5,6] Although this process is more straightforward, the high temperature required results in significant energy use. A more favourable alternative is the alkaline hydrothermal technique, which processes alumina-bearing materials under milder conditions. This method has also been applied to recover alumina from materials like coal fly ash through a two-stage alkaline leaching process.[7,8] In this system, NaOH is introduced as a liquid reagent to separate silica, while a combination of NaOH and CaO helps break down the fly ash. In hydrometallurgical processing, alumina must also be isolated from dissolved silica before sodium aluminate can precipitate.[7]

EXPERIMENTAL

Material

Napa Soil obtained from Pesisir Selatan, West Sumatra, Indonesia, hydrochloric acid (37% w/v, EMSURE® grade, Merck, Germany), sodium hydroxide (Merck, Germany), and aquabidest.

Instrumentation

The samples and synthesised products were analysed using several instruments, including Fourier Transform Infrared Spectroscopy (FTIR; PerkinElmer, Japan), X-ray Diffraction (XRD; X'PERT PRO PANalytical, Netherlands), X-ray Fluorescence (XRF; Epsilon3 PANalytical, Netherlands), Scanning Electron Microscopy coupled with Energy-Dispersive X-ray analysis (SEM-EDX; ZEISS, Germany), and Thermogravimetric Analysis (TGA; DTG-60 Shimadzu, Japan).

Napa Soil Preparation

Raw NS samples in the form of chunks and coarse grains were smoothed into fine grains using milling, then burned in the furnace at 750 °C for 4 hours. Characterisation using XRF was done before and after calcination to determine the composition of NS samples.

Silica Extraction

Samples of calcined NS were mixed until homogeneous with NaOH (w/w; 1:5) with a ratio of concentration 2.0, 4.0, 6.0, and 8.0 M, accompanied by heating at a temperature of 95°C for 2 hours using a magnetic stirrer for a constant stirring of 600 rpm. The obtained Na-silicate filtrate was added with 6.0 M HCl gradually at a pH range of 6.5-7. Subsequently, the silica gel was filtered and rinsed with distilled water to be further dried at 110°C for 3 hours. This helps to remove moisture content, and then calcination is conducted at 550°C for 2 hours to obtain SiO_2.

Alumina Extraction

Calcined NS samples were mixed with HCl using concentration variations of 1, 1.5, 2, and 2.5 M. They were then stirred with a magnetic stirrer at 95°C at a speed of 600 rpm for 2 hours until a slurry was formed. The making of $Al(OH)_3$ solution was carried out by mixing the leaching acid solution ($AlCl_3$) with NaOH 10 M at a speed of 600 rpm until the pH reached 4 - 6.5. Then, the resulting solution was placed in an oven at 110°C for 2 hours and calcined at 550 °C to obtain Al_2O_3.

RESULTS AND DISCUSSION

Calcination of NS at 750 °C converts the crystal phase into a reactive amorphous phase.[9] This process also increases the levels of alumina and silica. The differences in chemical composition of NS before and after calcination are shown in Table-1, where changes in oxide compound levels are attributed to the loss and transformation of compounds upon heating at high temperatures.

Table-1: NS Composition Before (NS 1) and after (NS 2) Calcination (%w/w)

Sample	SiO_2	Al_2O_3	Fe_2O_3	CaO	MgO	SO_3	K_2O	Na_2O
NS 1	59.38	28.78	3.96	0.37	1.08	0.13	1.38	0.2
NS 2	62.7	31.16	4.04	0.24	1.14	0.13	1.43	0.18

Silica Extraction

Silica readily dissolves in alkaline media and precipitates under acidic conditions. Increasing temperature enhances the reaction rate, while stirring improves interaction between the solvent and solute. Figure-1 shows the influence of NaOH concentration on SiO_2 extraction. As NaOH concentration increased, more SiO_2 was initially extracted. This is because NaOH dissociates to form Na^+ and OH^- ions, where the nucleophilic OH^- attacks Si in SiO_2. The double bond in the oxygen atom can break, producing SiO_2 OH^- and releasing H^+. Further bond breaking leads to SiO_3^{2-} formation. Dehydrogenation then occurs with the formation of water molecules (H_2O) from the bond between OH^- and H^+.[10] It was observed that at NaOH concentrations of 6 M and 8 M, the silica extraction yield decreased, indicating that the optimum condition for silica extraction was achieved at 4 M NaOH.

The reaction that occurred is as follows:

$SiO_{2(aq)} + 2NaOH_{(aq)} \rightarrow Na_2SiO_{3(aq)} + H_2O_{(aq)}$

$Na_2SiO_{3(aq)} + H_2O_{(l)} + 2HCl_{(aq)} \rightarrow Si(OH)_{4(aq)} + 2NaCl_{(aq)}$

$Si(OH)_{4(aq)} \rightarrow SiO_{2(s)} + 2H_2O_{(l)}$

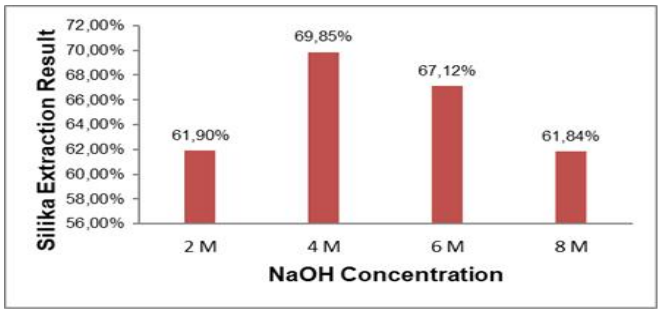

Fig.-1: Silica Mass Extracted Based on Variation in NaOH Concentration

Initially, the sodium silicate (Na_2SiO3) solution undergoes a filtration process to isolate the liquid filtrate from the remaining solid residue. The remaining solid is then treated with 6 M HCl for 24 hours to form silica gel, where HCl functions as a precipitating agent. Na^+ ions are exchanged with H^+ ions, producing silicic acid. The resulting sodium silicate solution is subsequently mixed with 1 M HCl and stirred with a magnetic stirrer until silica gel forms at a pH of approximately 6.5–7.0. At pH 7, silica formation is favoured because the introduction of HCl protonates siloxys groups ($Si–O^-$) into silanol groups (Si–OH). The increase in H^+ concentration from the added HCl encourages silanol formation. With HCl acting as a catalyst, the siloxys group ($O–Si–O^-$) then reacts with the silanol groups to produce siloxane bonds (Si–O–Si), as shown in Fig.-2. The resulting silica gel is then filtered, rinsed with distilled water, and dried at 110 °C for 3 hours to eliminate residual moisture. Finally, calcination at 550 °C for 2 hours converts the gel into fine SiO_2 powder.

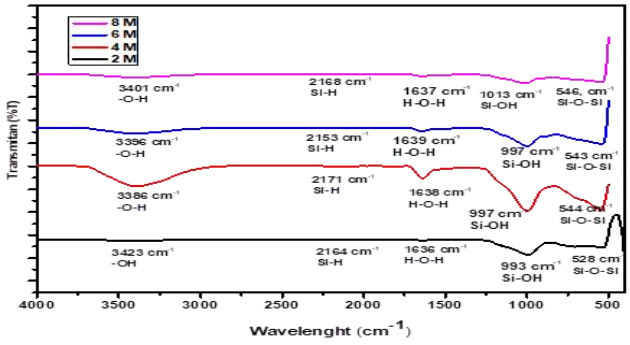

Fig.-2: Silica FTIR Analysis Results

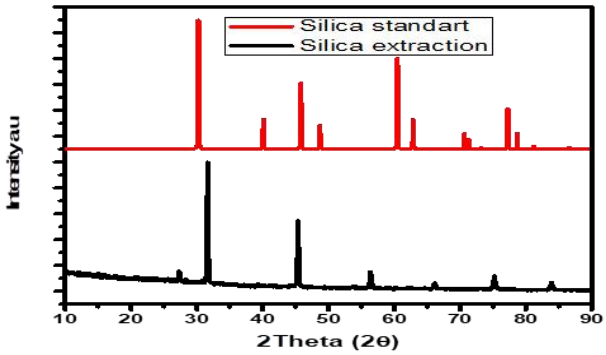

Fig.-3: Silica XRD Diffractogram

The results indicated that the extracted silica exhibited a crystalline phase, consistent with the standard ICSD 36226 (Fig.-3). Some of the peaks that appeared included 2θ = 27.29° ; 31.63 °; 45.38° ; 53.77 °; 56.41 °; 66.17° ; and 75.22° . The diffractogram pattern of NS samples found peaks at 2θ = 27.29° and 31.63°, which were indicated as SiO_2 with a crystalline phase as reported by Biswas *et al.* (2018).[11] The silica peak at an angle of 2θ = 27.29° indicates the quartz phase. The diffraction peak at 2θ = 31.63° corresponds to the cristobalite phase, as referenced in the Joint Committee on Powder Diffraction Standards (JCPDS) database.[12] The presence of silica is shown in the diffraction pattern that appears at an angle of 2θ = 13.67° to 2θ = 37.37°.[13] Furthermore, a strong diffraction peak was observed at 2θ = 45.38°, which corresponds to the diffraction pattern of aluminium oxide (Al_2O_3) as reported in the JCPDS database.[14] This result is also in line with XRF analysis, where there is still a certain amount of Al_2O_3 in the extracted silica. The XRF results confirmed there is still a certain amount of Al_2O_3 in silica extracted from NS (Table-2).

Table-2: XRF Silica Extraction Results

Element	Conc (%)	Compound	Conc (%)
Al	12,354	Al_2O_3	16,103
Si	58,875	SiO_2	69,856
P	1,638	P_2O_5	1,717
Cl	25,397	K_2O	0,283
K	0,588	CaO	0,34
Ca	0,613	TiO_2	0,005
Ti	0,008	V_2O_5	0,006
V	0,008	Cr_2O_3	0,001
Cr	0,001	Fe_2O_3	0,209
Fe	0,376	CuO	0,002
Cu	0,005	ZnO	0,035
Zn	0,072	Ga_2O_3	0,026
Ga	0,051	GeO_2	0,003
Ge	0,004	Cl	11,412

From the SEM results, it can be seen that he uneven morphology of the sample surface consists of clumps, some of which are spherical (Fig.-4). This indicates a fairly diverse size of silica particles, namely < 14-134 nm. The silica particles appear relatively large and irregular in shape, while the surface of the particles is rough and heterogeneous. Some visible voids between particles were also observed, suggesting a porous structure at the macroscopic level.

The results of the DTA-TGA analysis of pumice powder samples tend to be dominated by endothermic events accompanied by mass shrinkage (Fig.-5). Based on the figure, there is a decrease in the thermography curve as the heating temperature increases. Within the 31–61 °C temperature interval, the extracted silica sample gains mass owing to the evaporation of water molecules that bond to the sample and the evaporation of impurities adhering to the surface. Massa growth returns to 250°C as warming temperatures rise.

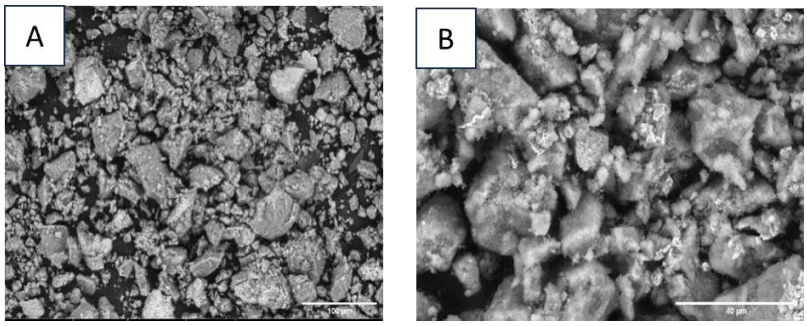

Fig.-4: SEM of silica with magnification a). 250x and b). 1000x

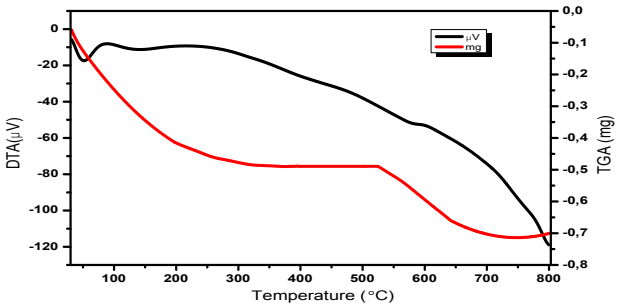

Fig.-5: TGA Silica Extracted using an Alkaline Solution

Alumina Extraction

The process of leaching acid to obtain aluminium chloride ($AlCl_3$) is carried out by reacting the hydrochloric acid solution (1.0, 1.5, 2.0 and 2.5 M) with NS. HCl was selected as a leaching agent because it did not react with SiO_2 and removed Si impurities in NS.

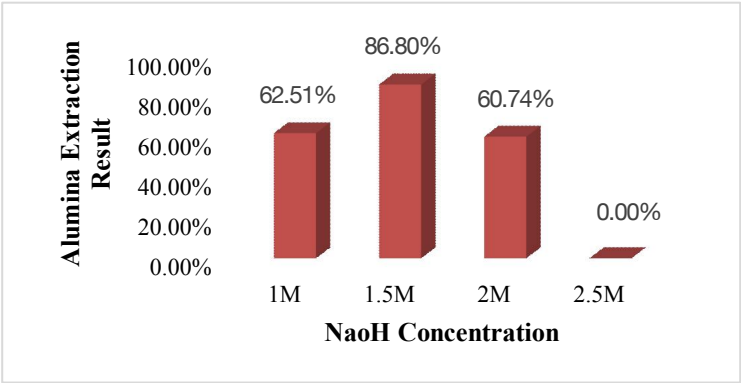

Fig.-6: Alumina Extraction from NS using HCl

At 1.5 M, extraction reached a maximum yield at 86.8% but decreased significantly at higher HCl concentration (Fig.-6). An increase in HCl concentration promotes greater silicate formation, which in turn reduces alumina extraction. The $AlCl_3$ -containing filtrate obtained from the acid extraction is then treated with 5 M sodium hydroxide (NaOH), requiring neutralisation to produce $Al(OH)_3$ precipitates. The equation for the formation of aluminium hydroxide from aluminium chloride is as follows:[15]

$$AlCl_{3(l)} + NaOH_{(l)} \rightarrow Al(OH)_3\downarrow + 3NaCl$$

$Al(OH)_3$ is formed in the range of $4.5 < pH < 6.5$, while the $pH \leq 4$ forms $Al(OH)_2^+{}_{(aq)}$. At $pH \leq 4$, the number of H^+ ions generated will increase, which results in the re-dissolution of $Al(OH)_3$ and shifts the equilibrium reaction toward the products. The dissolution of $Al(OH)_3$ and the equilibrium reaction shift towards the product. However, when the $pH > 6.5$ form $Al(OH)_4^-{}_{(aq)}$ is produced due to the more OH^- ions produced, then the equilibrium will shift towards the product. Calcination of $Al(OH)_3$ is then carried out at 550 °C for 2 hours to produce Al_2O_3 in the alkaline fusion stage.[7] The XRD analysis determines the

crystallinity and purity of the resulting alumina. This study aims to investigate the influence of hydrochloric acid (HCl) optimum concentration on the size of the alumina crystals produced. Typical peaks of alumina can be determined according to the Inorganic Crystal Structure Database (ICSD-28920). Figure-8 shows the XRD diffractogram of alumina with the 3 main peaks of alumina at an angle of 2θ = 35.27$^{o\circ}$, 43.50$^{o\circ}$, and 57.65$^{o\circ}$.

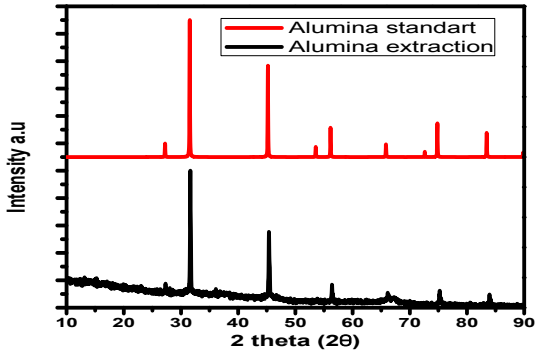

Fig.-7: Silica FTIR Analysis Results, XRD Diffractograms of Alumina

Alumina is produced through extraction derived from the soil material napa flavoured corundum α-Al_2O_3, which has a hexagonal crystal structure. The alpha alumina crystal structure is more stable and was produced. In the calcination stage, the octahedral layer is converted to hexagonal. Referring to the literature, alpha alumina has a hexagonal structure.[16] The alumina produced from the extraction of NS material has a corundum α-Al_2O_3 phase with a hexagonal crystal structure. The resulting alumina is expected to have a hexagonal structure, as shown in Fig.-6 below.

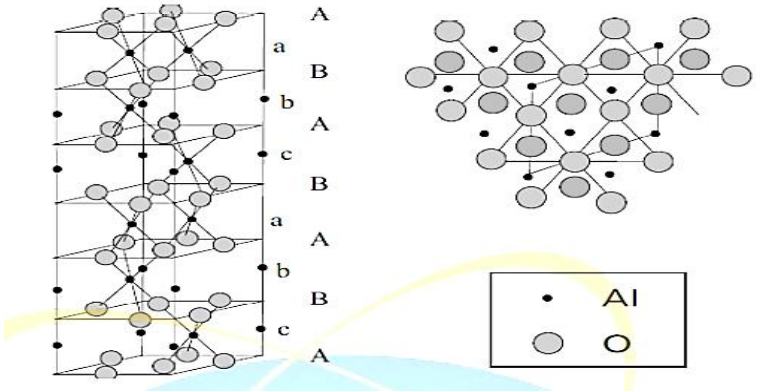

Fig.-8: Crystal Structure of α-Al_2O_3. [17]

Based on the differences between silica and alumina, the crystalline α-Al_2O_3 obtained a relatively good purity percentage of 95.6%. This is under the XRF data in Fig.-8 and Table-3, which shows that the extracted alumina has a dominant percentage over other oxide.

Table-3: Alumina XRF Results

Element	Conc (%)	Compound	Conc (%)
Na	0	Na_2O	0
Mg	2,351	MgO	3,082
Al	50,363	Al_2O_3	86,80
Si	0	SiO_2	0
P	0	P_2O_5	0
Cl	39,887	K_2O	0,604
K	0,982	CaO	1,938
Ca	2,739	MnO	0,016
Mn	0,025	Fe_2O_3	1,507
Fe	2,155	CuO	0,085

Cu	0,142	ZnO	0,147
Zn	0,247	As_2O_3	0,002
As	0,002	Rb_2O	0,003
Br	0,007	SrO	0,015
Rb	0,005	Y_2O_3	0,159
Sr	0,027	Ag_2O	0

The characterisation of FTIR is carried out to identify functional groups from alumina extraction results (Al_2O_3), where several absorption peaks appear in the IR spectrum. Wave numbers 4000-1250 cm^{-1} indicate the presence of vibration absorption bands of the group -OH that binds the Atom Al octahedral. The absorption bands at 3450, 3527, and 3620 cm^{-1} correspond to –OH stretching vibrations, while the band at 1639 cm^{-1} represents bending vibrations.[18] The stretch and band of –OH absorption are in the wave number area of 3448.72 cm^{-1} and 1635.64 cm^{-1}. [19]

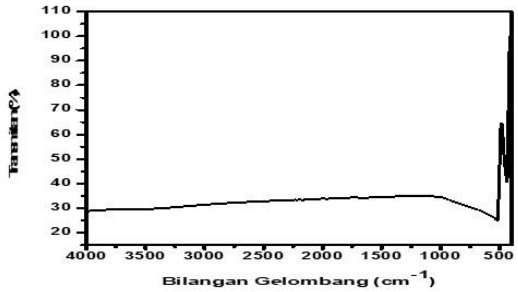

Fig.-9: FTIR Alumina Analysis Results

The wavenumber region of 3700–3400 cm^{-1} corresponds to the –OH group absorption peak from water molecules, indicating O–H stretching vibrations. The tendril vibration –OH peak of the water molecule also appears in the wave number regions 1635.34 cm^{-1} to 1635.64 cm^{-1}. Al-O tendril vibrations appear in wave numbers 850-650 cm^{-1} with a symmetrical range. The absorption in wave numbers between 1000-435 cm^{-1} states that the presence of a form of gamma alumina (γ-Al_2O_3) is located in 758 cm^{-1}, indicating the presence of a vibration bond of Al-O. In addition to the vibration of the tendrils, the peak of Al-O bending absorption is also found in the wave number area of 500 – 420 cm^{-1}, while the peak of absorption is 420-300 cm^{-1}, and open pores on the crystal were found.[20]

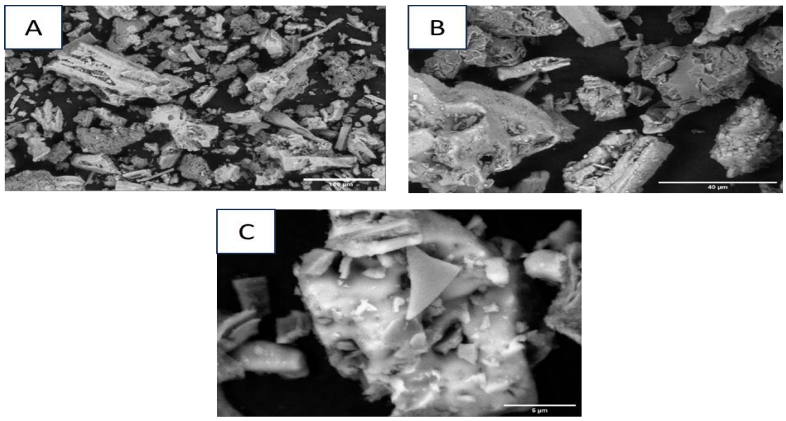

Fig.-10: Analysis of SEM Alumina Calcining at a Temperature of 750°C with Magnification a. 250 x, b. 1000 x, and c. 5000 x

Based on some literature, the peak of the vibration uptake of the tendrils and bends. Al-O is found in the area of waves 738 cm^{-1} and 620 cm^{-1}. [20,21] In other literature, the peak of IR absorption in the wave number area 775 cm^{-1} and 590 cm^{-1} is the vibration of the tendrils and bends of Al-O. Meanwhile, for the morphology analysis, the surface microstructure of the synthesised alumina crystal sample exhibits agglomeration to form a chunk with a porosity and the presence of tiny particles with the size of

nonhomogeneous granules, as determined by SEM examination. This agglomeration can appear due to the influence of calcination at a temperature of 750°C.

Thermal analysis of TGA alumina extraction results showed endothermic and exothermic peaks accompanied by mass loss, as presented in Fig.-10. Endothermal peaks occur at a temperature of 650 °C, indicating that the sample is dominated by water. This temperature also oxidises the rest of the organic group, resulting in a reduction in mass. The exothermal peak occurs at a temperature of 750 °C to form α-alumina.[22]

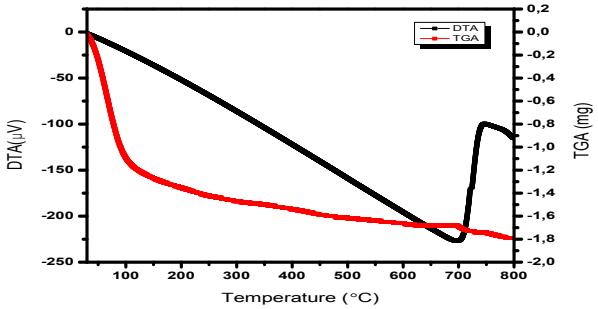

Fig.-11: Alumina TGA

CONCLUSION

This study successfully demonstrated an effective and sustainable method for extracting high-purity silica (SiO_2) and α-alumina (Al_2O_3) from Napa soil (NS) originating from West Sumatra, Indonesia. Through the combination of calcination, alkali fusion, and hydrothermal acid treatment, the crystalline phases in NS were converted into more reactive amorphous forms, significantly enhancing extraction efficiency. The optimum condition for silica extraction was achieved using 4 M NaOH, resulting in a silica product with 69.85% purity dominated by quartz and cristobalite phases. Meanwhile, the optimal extraction of alumina was obtained at 1.5 M HCl, yielding α-alumina with 86.8% purity and a stable corundum hexagonal structure. Characterisation using XRD, FTIR, SEM, XRF, and TGA confirmed the crystalline phases, functional groups, and morphological features of both materials, validating their structural integrity and high quality. These findings indicate that Napa soil is a valuable, low-cost, and eco-friendly precursor for producing advanced materials such as ceramics, catalysts, and adsorbents. Moreover, this research supports the principles of sustainable industrial development in alignment with SDG 9 and SDG 12 by promoting local resource utilisation and environmentally responsible material processing.

ACKNOWLEDGEMENTS

This research is funded by Universitas Negeri Padang with RKAT Fund, Decree Number 19/UN35/KU/2024 and contract number 1698/UN35.15/LT/2024

CONFLICT OF INTEREST

The authors declare no conflict of interest.

AUTHOR CONTRIBUTIONS

The present work is related to *SDG-9: Industry, Innovation and Infrastructure*. All the authors contributed significantly to this manuscript, participated in reviewing/editing and approved the final draft for publication. The research profile of the authors can be verified from their ORCID ids, given below:

Mawardi Mawardi http://orcid.org/0000-0001-5331-0748
Illyas Md Isa https://orcid.org/0000-0002-7621-2929
Syamsurizal https://orcid.org/0000-0001-5666-2669
Okta Suryani http://orcid.org/0000-0002-6825-9866
Fadlurrahman Mawardi http://orcid.org/0009-0007-8592-9191
Fiqrhatul Ilmi https://orcid.org/0009-0006-0847-4413
Salsabilla Yuswilia https://orcid.org/0009-0000-0475-0595
Feliska Amanda https://orcid.org/0009-0000-2681-3868

Cite this article as: M. Mawardi *et al.*, *Rasayan J. Chem.*, 19(1), 250-258(2026), https://doi.org/10.31788/RJC.2026.1919475.

REFERENCES

1. M. Mawardi, I. M. Isa, A. Ulianas, E. Sintiara, F. Mawardi, and R. Z. Putra, *Materials*, **14**, 13(2021), https://doi.org/10.3390/ma14133638
2. V. K. Yadav, and M. H. Fulekar, *Ceramics*, **3**, 3(2020), https://doi.org/10.3390/ceramics3030034
3. M. Sadat-Shojai, M. T. Khorasani, E. Dinpanah-Khoshdargi, A. Jamshidi, *Acta Biomaterial*, **9**, 8(2013), https://doi.org/10.1016/j.actbio.2013.04.012
4. A. Daulay, Andriayani, Marpongahtun, and S. Gea, *Rasayan Journal of Chemistry*, **14**, 3(2021), https://doi.org/10.31788/RJC.2021.1436351
5. L. S. Li, Y. S. Wu, Y. Y. Liu, and Y. C. Zhai, *The Chinese Journal of Process Engineering*, **11**, 2(2011).
6. A. A. Shoppert, I. V. Loginova, L. I. Chaikin, and D. A. Rogozhnikov, *KnE Material Science*, **2**, 2(2017), https://doi.org/10.18502/kms.v2i2.952
7. H. Li, J. Hui, C. Wang, W. Bao, and Z. Sun, *Hydrometallurgy*, **147-148**, 183(2014), https://doi.org/10.1016/j.hydromet.2014.05.012
8. S. Q. Su, J. Yang, H. W. Ma, F. Jiang, Y. Q. Liu, and G. Li, *Integrated Ferroelectric*, **128**, 1(2011), https://doi.org/10.1080/10584587.2011.576626.
9. M. R. Rowles, J. V. Hanna, K. J. Pike, M. E. Smith, and B. H. O'Connor, *Applied Magnetic Resonance*, **32**, 4(2007), https://doi.org/10.1007/s00723-007-0043-y
10. M. Spennato et al., *EFB Bioeconomy Journal*, **1**, 100008(2021), https://doi.org/10.1016/j.bioeco.2021.100008
11. R. K. Biswas, P. Khan, S. Mukherjee, A. K. Mukhopadhyay, J. Ghosh, and K. Muraleedharan, *Journal of Non-Crystalline Solids*, **488**, 1(2018), https://doi.org/10.1016/j.jnoncrysol.2018.02.037
12. B. T. Dipowardani, S. Sriatun, and T. Taslimah, *Jurnal Kimia Sains & Aplikasi*, **11**, 1(2008), https://doi.org/10.14710/jksa.11.1.20-28
13. V. H. Putranto, E. Kusumastuti, and Jumaeri, *Indonesian Journal of Mathematics and Natural Sciences*, **38**, 2(2015), https://doi.org/10.15294/ijmns.v38i2.5820
14. M. Gao, Q. Ma, Q. Lin, J. Chang, and H. Ma, *Material & Design*, **116**, (2017), https://doi.org/10.1016/j.matdes.2016.12.028
15. A. Ali, M. Al-Taie, and I. Ayoob, *Engineering and Technology Journal*, **37**, 4(2019), https://doi.org/10.30684/etj.37.4a.4
16. X. Jin, L. Gao, and J. Sun, *Journal of the American Ceramic Society,* **93**, 5(2010), https://doi.org/10.1111/j.1551-2916.2009.03544.x
17. T. Shirai, H Watanabe, M Fuji, and M. Takahashi, "Structural Properties and Surface Characteristics on Aluminum Oxide Powders," (2009).
18. S. Sushil, V. and S. Batra, *Applied Catalysis B: Environmental*, **81(1-2)**, 64(2008), https://doi.org/10.1016/J.APCATB.2007.12.002
19. P. S. Nayak, B. K. Singh, *Bulletin of Material Science*, **30**, 3(2007)
20. S. Sunardi, Y. Arryanto, and S. Sutarno, *Indonesian Journal of Chemistry*, **10**, 3(2010), https://doi.org/10.22146/ijc.21437
21. Z. Ramli and R. Saleh, *Malaysian Journal of Fundamental and Applied Science*, **4**, 2(2014), https://doi.org/10.11113/mjfas.v4n2.52
22. M. H. Basheet and F. K. Farhan, "Preparation and Characterisation of Bioceramic Cordierite for Medical Applications," (2021), https://doi.org/10.21203/rs.3.rs-934657/v1

[RJC-9475/2025]